ChemPubSoc Europe

DOI: 10.1002/open.201600128

Open Access ChemistryOPEN Full Papers

Plugging a Bipyridinium Axle into Multichromophoric Calix[6]arene Wheels Bearing Naphthyl Units at Different Rims

Guido Orlandini,[a] Giulio Ragazzon,[b] Valeria Zanichelli,[a] Lorenzo Degli Esposti,[b] Massimo Baroncini,[b] Serena Silvi,[b] Margherita Venturi,[b] Alberto Credi,*[c] Andrea Secchi,*[a] and Arturo Arduini[a]

Tris-(*N*-phenylureido)-calix[6]arene derivatives are heteroditopic non-symmetric molecular hosts that can form pseudorotaxane complexes with 4,4′-bipyridinium-type guests. Owing to the unique structural features and recognition properties of the calix[6]arene wheel, these systems are of interest for the design and synthesis of novel molecular devices and machines. We envisaged that the incorporation of photoactive units in the calixarene skeleton could lead to the development of systems the working modes of which can be governed and monitored by means of light-activated processes. Here, we report on the synthesis, structural characterization, and spectroscopic, photophysical, and electrochemical investigation of two calix[6]arene wheels decorated with three naphthyl groups anchored to either the upper or lower rim of the phenylureido calixarene platform. We found that the naphthyl units interact mutually and with the calixarene skeleton in a different fashion in the two compounds, which thus exhibit a markedly distinct photophysical behavior. For both hosts, the inclusion of a 4,4′-bipyridinium guest activates energy- and/or electron-transfer processes that lead to non-trivial luminescence changes.

1. Introduction

The suitable selection and design of molecular components are of paramount importance in determining the properties of molecular devices and to allow rational implementation of the mechanisms that govern their functions.[1–6] This is particularly true when these systems are supposed to perform a programmed task, such as, for example, sensing,[7,8] switching,[9–15] or nanoscale movements as in molecular machines.[16–18] Thus, a central factor to be considered during the design of new devices is how to connect, either covalently or non-covalently, and organize in space all the necessary molecular subunits, each of which should perform a predetermined function.[12,19,20] In this context, we have demonstrated that calix[6]arene **1** (Figure 1) acts as three-dimensional and heteroditopic wheel that, in low polarity media, forms oriented pseudorotaxanes and rotaxanes with dialkylviologen salts as axles.[21–23] A peculiar property of **1** is that suitable bipyridinium axles can unidirectionally transit through the calixarene annulus under the action of external stimulation.[24–27] Owing to the possibility of functionalizing the two chemically different rims, wheel **1** is also attractive as a scaffold for the construction of multicomponent species bearing covalently linked molecular subunits.

In view of our current interest in the design and synthesis of calix[6]arene prototypes of molecular machines, we envisaged that the incorporation of photoactive units in the calixarene skeleton could lead to the development of new systems the working modes of which can be governed and monitored through a wider set of control tools. The naphthyl moiety, which is extensively employed in supramolecular chemistry because of its rich and well-known photophysical behavior and its molecular recognition properties,[6,18,28–30] appears to be an ideal choice. Herein, we report the synthesis, structural characterization, and study of the spectroscopic, photophysical, and electrochemical behavior of two new calix[6]arene wheels decorated with three naphthyl groups anchored either to the upper or lower rim of the phenylureido calix[6]arene platform. We also describe their ability to form pseudorotaxane com-

[a] *Dr. G. Orlandini, V. Zanichelli, Prof. A. Secchi, Prof. A. Arduini*
Dipartimento di Chimica, Università degli Studi di Parma
Parco Area delle Scienze 17A, 43124 Parma (Italy)
E-mail: andrea.secchi@unipr.it

[b] *G. Ragazzon, L. Degli Esposti, Dr. M. Baroncini, Dr. S. Silvi, Prof. M. Venturi*
Dipartimento di Chimica "G. Ciamician"
and Interuniversity Center for the Chemical Conversion of Solar Energy
Bologna Unit, Università di Bologna
Via Selmi 2, 40126 Bologna (Italy)

[c] *Prof. A. Credi*
Dipartimento di Scienze e Tecnologie Agro-alimentari
Università di Bologna
viale Fanin 50, 40127 Bologna (Italy)
E-mail: alberto.credi@unibo.it

Supporting Information and the ORCID identification number(s) for the author(s) of this article can be found under http://dx.doi.org/10.1002/open.201600128.

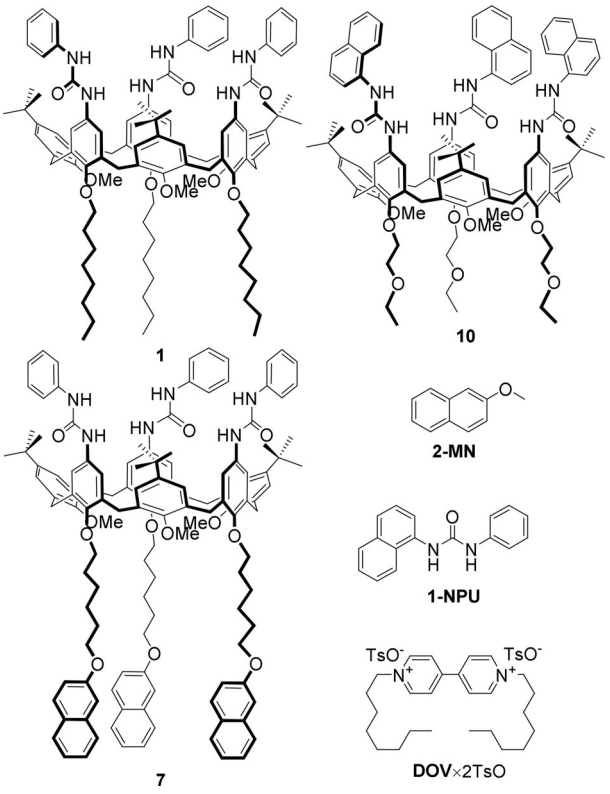

Figure 1. Calix[6]arenes-based "wheels" **1**, **7**, and **10**, model compounds **2-MN** and **1-NPU**, and the viologen-based "axle" **DOV**×2TsO used in this study.

plexes with a 4,4′-bipyridinium guest and the consequences of the complexation on their peculiar physicochemical properties.

2. Results and Discussion

2.1. Synthesis and Structural Characterization of the Wheels

To study whether the photophysical properties of the naphthalene unit can be affected by its location within a defined supramolecular system, we managed to synthesize the calix[6]-arene-based hosts **7** and **10** (Figure 1), which are characterized by the different positions of the three naphthyl units with respect to the aromatic cavity of the macrocycle. The three β-naphthyloxy groups of **7** are linked to phenolic groups present at the macrocycle lower rim through a C6 alkyl chain acting as a spacer, whereas in **10** these units are directly attached to the three urea moieties present on the host upper rim. As suggested by previous studies,[21–23,31,32] these two derivatives present all the structural features necessary to maintain their excellent recognition properties, in low-polarity solvents, towards molecular axles derived from the 1,1′-dialkyl-4,4′-bipyridinium (viologen) unit, namely, 1) a preorganized electron-rich aromatic cavity to stabilize the dicationic unit of the axle, and 2) ureido groups that, acting as hydrogen-bond donors, can interact with the counter anions of the axle.

Calixarene **7** was obtained through a convergent synthetic approach (Scheme 1); the naphthyl-containing alkylating agent

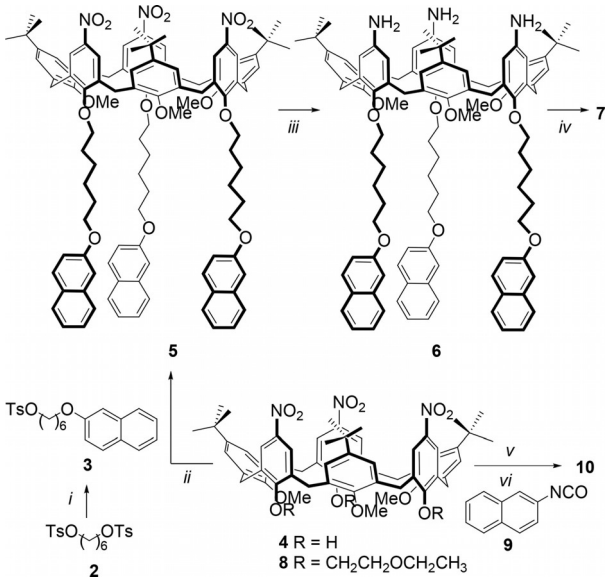

Scheme 1. Reagents and conditions: i) 2-naphthol, K_2CO_3, CH_3CN, reflux, 48 h, 72%; ii) K_2CO_3, CH_3CN, reflux, 72 h, 43%; iii) $NH_2NH_2{\cdot}H_2O$, Pd/C, MeOH, reflux, 6 h, 98%; iv) C_6H_5NCO, CH_2Cl_2, r.t., 2 h, 38%; v) $NH_2NH_2{\cdot}H_2O$, Pd/C MeOH, reflux, 6 h; vi) CH_2Cl_2, r.t., 2 h, 48%.

3 was obtained in high yield by reacting 2-naphthol with an excess of 1,6-hexanediol ditosylate (**2**) in acetonitrile at reflux. A similar procedure was adopted to functionalize the phenolic groups at the lower rim of the known calix[6]arene **4**,[33] to yield **5**. The nitro groups of **5** were then quantitatively reduced to amines in methanol at reflux by using hydrazine monohydrate as the reducing agent and Pd/C as the catalyst. The phenylureido moieties were finally introduced on the macrocycle upper rim by reacting **6** with phenyl isocyanate in dry dichloromethane to yield **7** with 16% overall yield. Calixarene **10** was synthesized in two steps starting from the known trinitro calix[6]arene derivative **8** (Scheme 1).[34] The nitro groups were quantitatively reduced by using the same route adopted for **5**. The resulting triamino derivative was not isolated but immediately reacted with 1-naphthyl isocyanate **9** to obtain **10** in 48% overall yield.

The ^{1}H NMR analysis of **7** reveals that this macrocycle adopts, on the NMR timescale in solutions of low-polarity solvents such as $CDCl_3$, CD_2Cl_2 (see the Supporting Information), and [D_6]benzene, a pseudo *cone* conformation in which the three alternate phenolic rings bearing the phenylureido units define a trigonal prism, whereas the remaining three, bearing the *tert*-butyl groups, are oriented with their methoxy groups pointing towards the center of the cavity. This geometrical arrangement generates few diagnostic signals such as the unusual upfield shift (approximately 2.9 ppm) of the resonance of the methoxy groups and the two doublets at $\delta = 4.4$ and 3.6 ppm ($^2J = 15.6$ Hz), related to the bridging methylene groups of the macrocycle. The ^{1}H NMR spectrum of **10** shows very broad resonances in $CDCl_3$ and [D_6]benzene (see Figure 2c), which is evidence for the higher mobility of this host with respect to **7**.

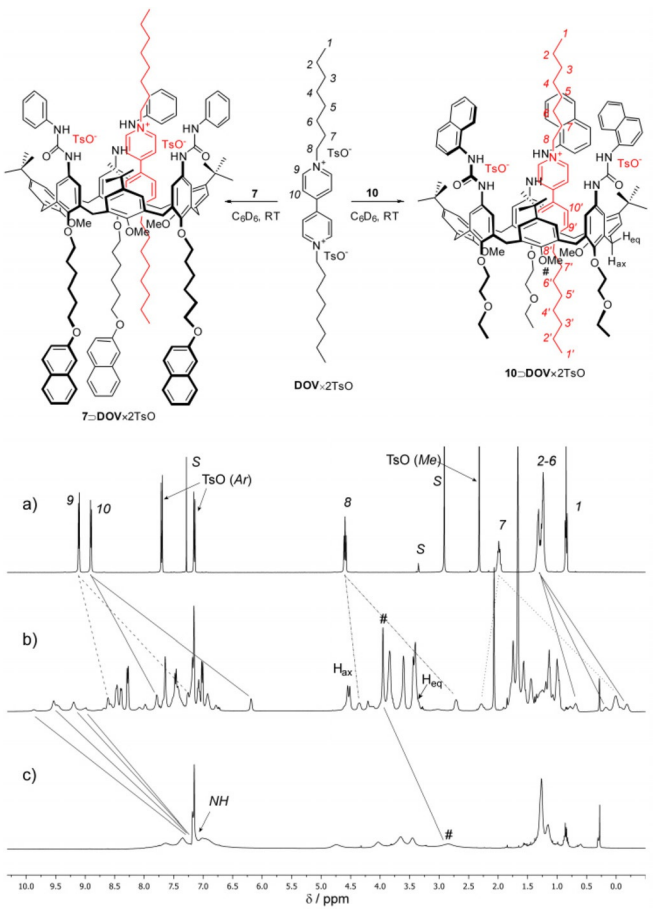

Figure 2. Top: Schematic representation of the formation of pseudorotaxanes **7**⊃**DOV**×2TsO and **10**⊃**DOV**×2TsO. Bottom: ^{1}H NMR (400 MHz) spectra of a) **DOV**×2TsO in $CDCl_3/CD_3OD$ (95:5), b) **10**⊃**DOV**×2TsO, and c) **10** in C_6D_6. The solid, dotted, and dashed lines indicate the most relevant shifts of the wheel and axle resonances upon formation of the pseudorotaxane complex; for the axle and wheel protons labeling, see the drawing above.

2.2. Preparation and Structural Characterization of the Pseudorotaxanes

The ability of wheels **7** and **10** to form pseudorotaxanes with 4,4′-bipyridinium axles in low-polarity solvents was evaluated by ^{1}H NMR, UV/Vis, and luminescence spectroscopy (see below). NMR measurements were carried out in [D_6]benzene solution by mixing wheel **7** or **10** with a molar excess of dioctylviologen ditosylate (**DOV**×2TsO). The mixtures were stirred at room temperature until the color of the solution changed from yellowish to ruby red. The undissolved viologen salt was then removed by filtration, and the resulting homogeneous solution was subjected to NMR analysis (see Figure 2 and Supporting Information). According to our previous studies carried out on similar systems,[21,27,31] the presence of several diagnostic signals in the spectra confirmed the formation of a 1:1 complex with pseudorotaxane topology. For example, in the ^{1}H NMR spectrum of **10**⊃**DOV**×2TsO (Figure 2b) it can be observed that the methoxy groups resonate as a sharp singlet at $\delta = 3.95$ ppm, thus significantly shifted to lower fields ($\Delta\delta \approx 1.1$ ppm) with respect to the same signal in the free wheel (Figure 2c). The same behavior was observed for the complex containing wheel **7** (see the Supporting Information). These findings suggest that the methoxy groups of both **7** and **10** are no longer affected by the shielding of the aromatic cavity because of the threading of the axle into the macrocycle. Another symptomatic observation is the large downfield shift (approximately 3 ppm) experienced by the protons of the ureido groups (NH) located at the upper rim of the hosts (see Figure 2b). This shift is consistent with the participation of the ureido groups in the complexation process by binding the counter anions of the axle. Other evidence for the pseudorotaxane formation were gathered by monitoring the chemical shift of the signals of the axle (Figure 2a), in particular those corresponding to the aromatic and N–CH_2 protons (8), which experience a noticeable upfield shift (up to 2.5 ppm) caused by the strong shielding effect exerted by the aromatic cavity of the calix[6]arene. It is important to note that in both pseudorotaxane complexes, the calix[6]arene hosts maintain their pseudo *cone* conformation on the NMR timescale. This arrangement is witnessed by the presence in the spectra (see Figure 2b and the Supporting Information) of the typical AX system of two doublets relative to the protons belonging to the hosts methylene bridging units at approximately 4.5 and 3.5 ppm (H_{ax} and H_{eq} in Figure 2b). The latter is overlapped with other calixarenes resonances, but it can be easily identified through 2D NMR measurements (see the Supporting Information).

2.3. Spectroscopic and Photophysical Experiments on Wheel 7 and its Pseudorotaxane 7⊃DOV×2TsO

The absorption and luminescence data for the calixarene host **7**, the guest **DOV**, their pseudorotaxane complex **7**⊃**DOV**×2TsO, and the model compounds for the calixarene scaffold (**1**) and for the naphthalene chromophore (2-methoxynaphthalene, **2-MN**) are reported in Table 1.

The UV/Visible absorption spectra of **7** in CH_2Cl_2 (Figure 3) show the typical bands of the aromatic systems of the calixarene skeleton in the 240–300 nm region, whereas the features occurring between 280 and 340 nm are assigned to π–π* transitions of the 2-alkoxynaphthalene units at the macrocycle lower rim. The absorption spectrum of **7** matches well with

Table 1. Absorption and luminescence data for the calixarene host **7**, the guest **DOV**, their pseudorotaxane **7**⊃**DOV**×2TsO complex, and the model compounds for the chromophoric units (air-equilibrated CH_2Cl_2, room temperature).

Compound	Absorption		Luminescence		
	λ_{max} [nm]	ε [$M^{-1}cm^{-1}$]	λ_{max} [nm]	Φ	τ [ns]
1[a]	250[b]	60 000[b]	340	0.0025	< 1[c]
2-MN	327	1900	348	0.12	4.8
7	327	5200	350	0.12	5.0
	250[b]	63 000[b]			
DOV×2TsO	270	24 000	–	–	–
7⊃**DOV**×2TsO	460	600	350	0.006	< 1[c]

[a] Data from Ref. [23]. [b] Shoulder on the lower energy side of an intense band. [c] The lifetime value is shorter than the time resolution of the equipment.

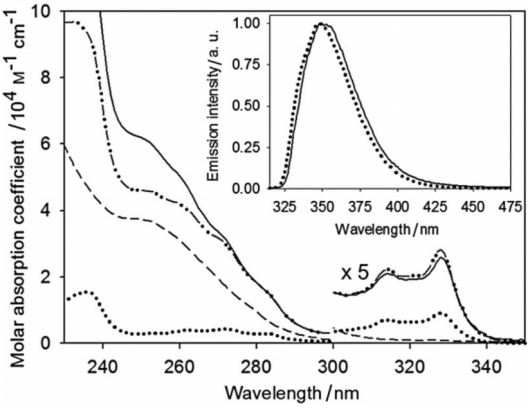

Figure 3. Absorption spectra of multichromophoric calixarene **7** (full line), calix[6]arene **1** (dashed line), and **2-MN** (dotted line). The sum of the absorption spectra of the chromophoric components of **7** (dashed dotted line) is also shown for comparison. Inset: normalized emission spectra ($\lambda_{exc}=315$ nm) of **7** (full line) and **2-MN** (dotted line). Conditions: air equilibrated CH_2Cl_2, room temperature.

the sum of the absorption spectra of its chromophoric components (**1** plus 3×**2-MN**) in the 280–340 nm region, indicating the absence of interactions between the pendant naphthalene units in the ground state. On the other hand, the absorption of **7** is substantially more intense than the sum of its chromophoric components in the 240–280 nm region. As the naphthalene units and the wheel skeleton are electronically insulated by the long alkyl chains, we hypothesize that the change in the calixarene absorption bands arises from conformational effects exerted on the diphenylureido units of the wheel by the bulky substituents at the lower rim. In CH_2Cl_2 at room temperature, compound **7** shows a luminescence band ($\lambda_{max}=350$ nm) that is safely assigned to the fluorescence of the alkoxynaphthalene units (Table 1 and Figure 3, inset). The emission quantum yield ($\Phi=0.12$) and lifetime ($\tau=5.0$ ns) values are identical within errors to those of the **2-MN** model. In a rigid matrix at 77 K, **7** shows both the structured fluorescence ($\lambda_{max}=$ 350 nm) and phosphorescence ($\lambda_{max}=465$ nm) bands of the alkoxynaphthalene units (see the Supporting Information). The corrected excitation spectrum[35] of **7** ($\lambda_{em}=350$ nm) at room temperature matches with the absorption spectrum of the same compound only between 310 and 340 nm, whereas it is significantly weaker in the 230–310 nm region. Conversely, the excitation spectrum of **7** exhibits a good overlap with the absorption spectrum of **2-MN** in the whole spectral region monitored (see the Supporting Information).

This observation indicates that the energy transfer from the excited states located on the calixarene skeleton to the excited singlet level of the pendant naphthalene units is inefficient. Unfortunately, an estimation of the residual fluorescence intensity arising from the calixarene annulus ($\lambda_{max}=340$ nm, Table 1) is prevented because such an emission band is covered by the much more intense naphthalene-type fluorescence ($\lambda_{max}=$ 350 nm). The application of the Förster model[36,37] suggests that the low energy-transfer efficiency is determined by the very poor overlap between the calixarene-type (donor) emission and the naphthalene-type (acceptor) absorption, together with the small quantum yield of the calixarene-type emission. In summary, the naphthalene units appended at the lower rim of the wheel as in **7** are photophysically independent both of one another and of the calixarene chromophore.

The addition of **DOV**×2TsO to a solution of **7** causes changes in the UV absorption bands of the molecular components and the appearance of broad absorption features in the 350–600 nm region ($\lambda_{max}=460$ nm, Table 1), arising from charge-transfer (CT) interactions between the π-electron-rich aromatic units of the calixarene and the π-electron-poor 4,4′-bipyridinium moiety of the guest (see the Supporting Information).[23,24,26,27] In the same experiment, the fluorescence band of **7** is quenched as a function of the amount of **DOV**×2TsO added (Figure 4). The absorption and luminescence data col-

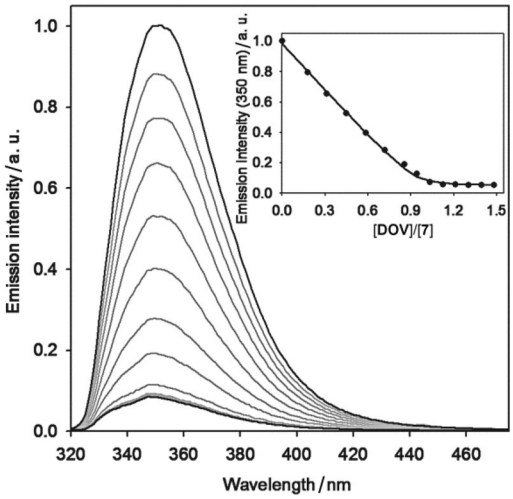

Figure 4. Luminescence spectral changes ($\lambda_{exc}=315$ nm) upon addition of increasing amounts of **DOV**×2TsO to a 3.0×10^{-5} M solution of **7**. The inset shows the titration curve obtained by plotting the emission intensity at 350 nm as a function of the **DOV**×2TsO equivalents; the full line is the data fitting corresponding to a 1:1 binding model. Conditions: air-equilibrated CH_2Cl_2, room temperature.

lected in the titration experiments could be satisfactorily fitted with a 1:1 binding model, yielding a value of the association constant $\log K=7.0\pm0.2$. These results are consistent with the NMR data and with previous observations on related compounds,[23,24,26,27] and confirm the formation of a pseudorotaxane in which **DOV**×2TsO is threaded into the cavity of **7** with its bipyridinium unit located close to the aromatic units of the calixarene.

In the light of these observations, it is worth discussing the effect of the **DOV**×2TsO guest on the photophysics of the calixarene. From the residual emission intensity of **7** at the end of the titration, one can calculate the quenching rate constant according to Equation (1):

$$k_q = 1/\tau_0\,(\Phi_0/\Phi - 1) \qquad (1)$$

where τ_0 and Φ_0 are the luminescence lifetime and quantum yields of **7** in the absence of **DOV**×2TsO, and Φ is the luminescence quantum yield of the complex. According to the

data listed in Table 1, $k_q = 3.8 \times 10^9\ s^{-1}$. The quenching of the naphthalene-type emission of **7** by **DOV**×2TsO can involve two distinct mechanisms: mechanism i) energy transfer from the singlet excited state localized on an alkoxynaphthalene unit to the lower lying charge-transfer levels as a result of the calixarene–bipyridinium interaction, and mechanism ii) electron transfer from the alkoxynaphthalene singlet excited state to the encapsulated bipyridinium unit. Because of the good overlap between the naphthalene emission and the visible charge-transfer absorption and the large luminescence quantum yield of the donor, the Förster radius (i.e. the donor–acceptor distance at which the energy-transfer efficiency is 50%) is as long as 5.4 nm. Considering that the maximum distance between the naphthalene substituents and the center of the calixarene cavity is 1.5 nm, the energy-transfer process (mechanism i) is expected to be very efficient. Moreover, from the available excited-state energy and the potential values for oxidation of the donor and reduction of the acceptor (see above), one can estimate that the photoinduced electron transfer (mechanism ii) is highly exergonic ($\Delta G^\circ < -1.8$ eV).[38]

To gain more insight into the luminescence quenching mechanism, we performed emission experiments in a rigid matrix at 77 K. Under these conditions, the solvent reorganization energy is small and highly exergonic electron-transfer processes such as that mentioned above, which may fall into the Marcus inverted region, can become slow.[37,39] Both the naphthalene-type fluorescence and phosphorescence bands observed for **7** in CH_2Cl_2/$CHCl_3$ 1:1 at 77 K are absent in the spectrum of the **7**⊃**DOV**×2TsO complex (see the Supporting Information). The occurrence of such a strong quenching in a rigid medium at low temperature is consistent with an energy transfer from the naphthalene excited singlet to the charge-transfer (CT) levels. Laser flash photolysis experiments with ns excitation pulses, carried out in solution at room temperature, revealed no trace of the bipyridinium radical cation, which would be a product of the electron-transfer reaction. It cannot be excluded, however, that a fast back-electron transfer process prevents the accumulation of the bipyridinium radical cation on the ns timescale.

2.4. Spectroscopic and Photophysical Experiments on Wheel 10 and its Pseudorotaxane 10⊃DOV×2TsO

The absorption and luminescence data for the calixarene host **10**, the pseudorotaxane **10**⊃**DOV**×2TsO, and the model chromophoric compound for the calixarene (*N*-1-naphthyl-*N*′-phenylurea, **1-NPU**) are reported in Table 2. The absorption spectrum of **10** in CH_2Cl_2 (Figure 5) shows the bands typical of the naphthyl-phenylureido chromophore in the near UV region. The spectrum is very similar to the sum of the spectra of its chromophoric components (3×**1-NPU**), which suggests that the interactions between the pendant naphthalene units are negligible in the ground state.

The luminescence band of **10** in CH_2Cl_2 at room temperature is less intense, much broader, and shifted to longer wavelengths in comparison with that of the **1-NPU** model (Table 2 and Figure 5, inset). The excitation spectrum of **10** (λ_{em} = 410 nm, see the Supporting Information) is similar to its absorption spectrum. The emission band, however, shows a biexponential decay with $\tau_1 = 2.8$ ns and $\tau_2 = 18$ ns. The shorter lifetime is comparable with that of **1-NPU** ($\tau = 1.6$ ns) and its contribution to the overall decay decreases as the monitored emission wavelength is moved towards the lower energy side (Figure 5, inset). Based on these observations and in the light of the structure of **10**, it can be concluded that its emission has a dual nature: a higher energy and shorter lived component assigned to the individual naphthyl-phenylureido chromophores, and a lower energy and longer lived component attributed to the formation of excimers between the pendant naphthalene moieties. This hypothesis is confirmed by the fact that in rigid matrix at 77 K, in which the formation of excimers is prevented, both the fluorescence ($\lambda_{max} = 360$ nm) and phosphorescence ($\lambda_{max} = 540$ nm) bands of **10** coincide with those of **1-NPU** (see the Supporting Information).

The addition of **DOV**×2TsO to a solution of **10** causes absorption spectral changes consistent with the formation of a 1:1 complex, as discussed above for host **7**. In particular, a weak shoulder on the lower energy side of the more intense UV bands, assigned to calixarene–bipyridinium CT interactions,

Table 2. Absorption and luminescence data for the calixarene host **10**, the pseudorotaxane **10**⊃**DOV**×2TsO complex, and the model chromophoric compound **1-NPU** (air-equilibrated CH_2Cl_2, r.t.).

Compound	Absorption		Luminescence		
	λ_{max} [nm]	ε [$M^{-1}cm^{-1}$]	λ_{max} [nm]	Φ	τ [ns]
1-NPU	290	6900	360	0.18	1.6
10	295	24000	410	0.11	2.8[a] 18[a]
10⊃**DOV**×2TsO	450[b]	200[b]	360	0.017	1.5[a] 3.4[a]

[a] Biexponential decay. [b] Shoulder on the lower energy side of an intense band.

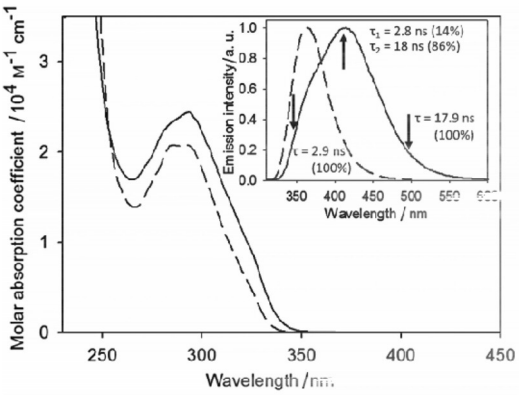

Figure 5. Absorption spectrum of calixarene **10** (full line) and sum of the absorption spectra of its **1-NPU** chromophoric components (dashed line). Inset: normalized emission spectra ($\lambda_{exc} = 300$ nm) of **10** (full line) and **1-NPU** (dashed line). Luminescence lifetime values measured at selected emission wavelengths, indicated by the arrows, are listed together with their respective contribution to the decay. Conditions: air-equilibrated CH_2Cl_2, room temperature.

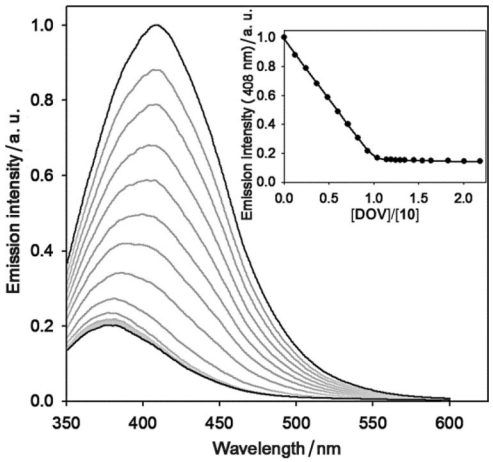

Figure 6. Luminescence spectral changes ($\lambda_{ex}=330$ nm) upon addition of increasing amounts of **DOV**×2TsO to a 4.0×10^{-6} M solution of **10**. The inset shows the titration curve obtained by plotting the emission intensity at 408 nm as a function of the **DOV**×2TsO equivalents; the full line is the data fitting corresponding to a 1:1 binding model. Conditions: air-equilibrated CH_2Cl_2, room temperature.

is observed (Table 2 and the Supporting Information). The emission changes of **10** upon titration with **DOV**×2TsO (Figure 6) consist of a decrease in the band intensity accompanied by a change in shape; namely, the band becomes sharper and its maximum exhibits a blueshift. From the titration curves obtained from absorption and luminescence data and fitted with a 1:1 binding model, a lower limiting value of the association constant log $K>7.5$ was obtained. Once again, these findings are consistent with the NMR results and confirm that **DOV**×2TsO is threaded into wheel **10** in a pseudorotaxane fashion. Notably, at the end of the titration, the shape of the residual emission band of the calixarene is very similar to that of **1-NPU** but its decay is still described by a biexponential function (Table 2). As observed for the uncomplexed calixarene **10**, the contribution of the two lifetime components to the overall decay depends on the observation wavelength: the weight of the longer lifetime increases at lower energies. On the basis of the discussion made for **10**, we assign τ_1 (1.5 ns) and τ_2 (3.4 ns) to emission from the naphthalene monomer and excimer species, respectively, in the complex. Both lifetimes are shorter than the corresponding values measured for **10** (Table 2), indicating that both the excited monomer (singlet) and dimer (excimer) levels are quenched in the presence of **DOV**×2TsO. The similarity of the luminescence band of the **10**⊃**DOV**×2TsO complex with that of the **1-NPU** model, which arises from a substantial disappearance of the contribution from the excimer emission, is consistent with the presence of a specific quenching pathway involving the excimers. It can also be hypothesized that the alkyl tail of the threaded **DOV**×2TsO guest can hinder the approach of two nearby naphthalene units by increasing the steric crowding at the upper rim of the calixarene, thus discouraging the formation of excimers.

As previously discussed for **7**, the emission quenching mechanism of **10** upon complexation with **DOV**×2TsO can be an energy transfer from the excited naphthyl-type units (monomers or dimers) to lower lying charge-transfer states owing to the calixarene–bipyridinium interaction, and/or an electron transfer from the excited naphthalenes to the bipyridinium guest, which is highly exergonic also in the case of **10**. In contrast with the results obtained for host **7**, the emission spectra of the **10**⊃**DOV**×2TsO complex at 77 K exhibit the fluorescence and phosphorescence bands of **10** (see the Supporting Information). Unfortunately, the luminescence intensities measured in the frozen solvent cannot be quantitatively compared and on the basis of our data we cannot extend the discussion any further.

2.5. Electrochemical Experiments

The association of the calixarenes with **DOV**×2TsO can also be probed by electrochemical techniques. The voltammetric patterns of hosts **7** and **10** in CH_2Cl_2 exhibit no reduction processes and several chemically irreversible oxidation processes with onset at about +1.1 V versus the saturated calomel electrode (SCE), assigned to the oxidation of the naphthalene units and the alkoxybenzene rings of the calixarene skeleton. Because of their irreversible nature, these processes will not be further discussed. **DOV**×2TsO shows the typical reversible monoelectronic reductions of the 4,4′-bipyridinium unit ($E_{1/2}{}'=-0.27$ V, $E_{1/2}{}''=-0.81$ V versus SCE, see Figure 7 and the Supporting Information) and no oxidation.[40] The inclusion of **DOV**×2TsO

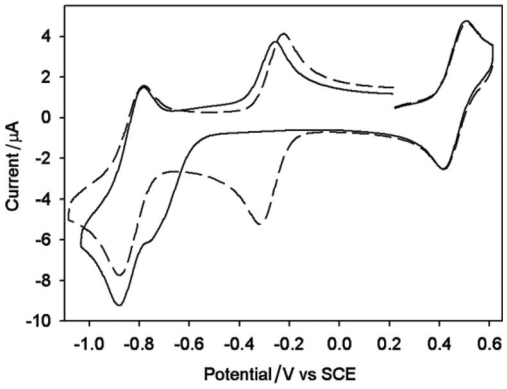

Figure 7. Cyclic voltammograms recorded upon reduction of **DOV**×2TsO (approximately 4.0×10^{-4} M) in the absence (dashed line) and in the presence (full line) of 1.5 equivalents of calixarene **10** to ensure full complexation of the electroactive guest. The wave at +0.460 V versus the SCE is due to ferrocene used as an internal standard. Conditions: argon-purged CH_2Cl_2, 0.04 M tetrabutylammonium hexafluorophosphate, scan rate 200 mV s^{-1}.

into either **7** or **10** causes a large negative shift of the first reduction potential, although the second process occurs at the same potential as for the free guest (see Figure 7 and the Supporting Information). These results indicate that 1) the bipyridinium unit becomes more difficult to reduce because it is stabilized inside the calixarene wheel, and 2) the one-electron reduction of **DOV**×2TsO promotes its dethreading from the host, in line with the behavior of several related bipyridinium-containing pseudorotaxanes.[23,25,41–43] The large peak-to-peak separation and the scan-rate dependence of the first reduction

process of the **7**⊃**DOV**×2TsO and **10**⊃**DOV**×2TsO complexes indicate that the complexation/decomplexation reactions occur on the voltammetric timescale; these aspects have been discussed in detail elsewhere.[23]

3. Conclusions

We have reported the synthesis, structural characterization, and study of the spectroscopic, photophysical, and electrochemical behavior of two new calix[6]arene wheels **7** and **10** decorated with three naphthyl groups anchored either to the upper or lower rim of the phenylureido calix[6]arene platform. We also describe their ability to form pseudorotaxane complexes with a 4,4′-bipyridinium guest (**DOV**×2TsO) and the consequences of the complexation on their peculiar physicochemical properties. In particular, in the case of calixarene **7**, the three naphthyl units connected to the lower rim do not interact with each other in the ground or excited states, and do not exchange electronic energy with the calixarene skeleton. The presence of a **DOV**×2TsO guest inside the wheel, however, enables photoinduced energy and/or electron-transfer processes to occur from the peripheral chromophores to the cavity. The behavior of calixarene **10**, in which the three naphthalene moieties are linked to the ureidic moieties at the upper rim, is markedly different. The naphthyl units do not exhibit significant interactions in the ground state but they can form excimer species characterized by a redshifted luminescence band and a longer lifetime. The threading of **DOV**×2TsO into the calixarene can activate energy- and/or electron-transfer pathways that cause the quenching of both the monomeric and, to a relatively higher extent, the excimeric naphthyl-type emission of **10**. For both calixarenes, the bipyridinium guest can be reversibly dethreaded/rethreaded from the host by reduction/oxidation of **DOV**×2TsO in a potential region in which the host is not electroactive, thus providing a way to modulate the photophysical properties of the multichromophoric calixarenes by means of electrochemical stimuli.

The investigated systems constitute a compelling example of the potential of calix[6]arenes for arranging functional molecular units with precise structural control around an efficient three-dimensional host. The resulting multicomponent species are of interest for the construction of novel molecular devices, machines, and motors that can take particular advantage of the topologically and chemically different rims of the calixarene cavity.

Experimental Section

General

NMR spectra were recorded by using the residual solvent signal as an internal reference. Melting points are uncorrected. Mass analyses were carried out in the ESI mode. Axle **DOV**×2TsO,[21] compound **2**,[44] calix[6]arenes **1**,[34] **4**,[33] and **8**[34] were synthesized according to literature procedures. All the other reagents were of reagent grade quality obtained from commercial suppliers and were used without further purification. Deuterated benzene was used as the solvent in most NMR experiments because a better resolution of the signals, especially in the low-field portion of the spectra, is afforded. Absorption and luminescence spectra were recorded at room temperature with a PerkinElmer lambda45 spectrophotometer and LS55 spectrofluorometer by using 1 cm quartz cuvettes. Emission spectra at 77 K were obtained from a frozen solution contained in a quartz tube immersed in a quartz Dewar filled with liquid nitrogen. Luminescence lifetimes were measured with an Edinburgh Instrument FLS920 time-correlated single-photon counting equipment. Luminescence quantum yields were determined by the optically dilute method by using naphthalene in air-equilibrated cyclohexane ($\Phi_L = 0.036$) as a standard.[45] Spectroscopic titrations were performed by adding small aliquots (typically 20 μL) of a concentrated solution of **DOV**×2TsO to a dilute solution of the calixarene. The titration curves were fitted according to a 1:1 association model by using the SPECFIT software.[46] Cyclic voltammetric experiments were carried out at room temperature in Ar-purged dichloromethane with an Autolab30 multipurpose instrument interfaced to a PC. A glassy carbon working electrode, a Pt wire counter electrode, and an Ag wire pseudoreference electrode were employed; ferrocene ($E_{1/2} = +0.460$ V versus SCE)[47] was present as an internal standard. The concentration of the compounds under examination was between 3×10^{-4} and 5×10^{-4} M; tetrabutylammonium hexafluorophosphate (0.03 to 0.05 M) was the supporting electrolyte. The potential scan rate was typically varied from 0.02 to 1 $V s^{-1}$.

Synthesis of 6-(Naphthalen-2-yloxy)hexyl tosylate (3)

In a 250 mL round-bottom flask, K_2CO_3 (2.9 g, 20.8 mmol) was added to a solution of 2-naphthol (1.5 g, 10.4 mmol) and 1,6-hexanediol ditosylate **2** (13.3 g, 31.2 mmol) in CH_3CN (100 mL). The resulting heterogeneous reaction mixture was heated at reflux for 36 h. After cooling to room temperature, the solvent was evaporated to dryness under reduced pressure and the sticky residue was taken up with ethyl acetate (100 mL). The resulting organic phase was washed with a 10% w/v solution of HCl (100 mL) and twice with distilled water (2×100 mL), then dried with anhydrous sodium sulfate and evaporated to dryness under reduced pressure. The oily residue was purified by column chromatography on silica gel (*n*-hexane/ethyl acetate 7:3) to yield 3.0 g of **3** (72%) as a white solid. M.p. = 71–72 °C; ^{1}H NMR ($CDCl_3$, 400 MHz): $\delta = 7.80$ (d, 2H, $J = 7.6$ Hz), 7.46 (t, 2H, $J = 8.0$ Hz), 7.36 (d, 2H, $J = 7.6$ Hz), 7.28 (s, 1H), 7.14 (d, 1H, $J = 7.2$ Hz), 4.10–4.05 (m, 4H), 2.41 (s, 3H), 1.76 (q, 2H, $J = 9.2$ Hz), 1.68 (q, 2H, $J = 9.2$ Hz), 1.52–1.44 ppm (m, 4H); ^{13}C NMR (100 MHz): $\delta = 157.0$, 144.7, 134.6, 133.2, 129.8, 129.3, 128.9, 127.9, 127.6, 126.7, 126.3, 123.5, 118.9, 106.6, 70.5, 67.7, 29.0, 28.8, 25.5, 25.2, 21.6 ppm; MS (ESI) *m/z*: 421.3 $[M+Na]^+$; elemental analysis calcd (%) for $C_{23}H_{26}O_4S$: C 69.32, H 6.58; found: C 69.28, H 6.60.

Synthesis of Calix[6]arene (5)

In a 100 mL sealed glass autoclave, a heterogeneous mixture of compounds **4** (0.8 g, 0.8 mmol), **3** (1.0 g, 2.5 mmol), and K_2CO_3 (0.5 g, 3.7 mmol) in CH_3CN (60 mL) was heated at reflux under vigorous stirring for 72 h. After cooling to room temperature, the solvent was evaporated to dryness under reduced pressure. The solid residue was taken up with ethyl acetate (80 mL) and the resulting organic phase washed with a 10% w/v solution of HCl (80 mL) and water (2×80 mL). The separated organic phase was dried over anhydrous sodium sulfate, filtered to remove the drying agent, and the solvent evaporated to dryness under reduced pressure. The residue was purified by column chromatography on silica gel

(hexane/ethyl acetate 8:2) to yield 0.58 g of **5** (43%) as a pale-yellow solid. M.p. = 108–109 °C; ^{1}H NMR ($CDCl_3$, 400 MHz): δ = 7.78–7.68 (m, 15H), 7.44 (dt, 3H, J_1 = 7.2, J_2 = 1.2 Hz), 7.33 (dt, 3H, J_1 = 7.2, J_2 = 1.2 Hz), 7.2 (bs, 3H), 7.14 (d, 3H, J = 2.4 Hz), 7.12 (s, 6H), 4.4 (bs, 6H), 4.09 (t, 6H, J = 6.4 Hz), 3.9 (bs, 6H), 3.6 (bs, 6H), 2.89 (s, 9H), 1.9 (bs, 12H), 1.63 (m, 12H), 1.32–1.25 ppm (m, 27H); ^{13}C NMR (100 MHz): δ = 159.9, 157.0, 154.4, 146.9, 143.7, 135.7, 134.6, 132.2, 129.3, 128.9, 128.0, 127.8, 127.6, 127.3, 126.7, 126.3, 125.5, 123.5, 123.2, 119.0, 106.5, 73.8, 67.7, 59.9, 34.3, 31.5, 31.0, 30.3, 30.2, 30.1, 29.7, 29.4, 29.2, 26.1, 25.9 ppm; MS (ESI) *m/z*: 1684.1 $[M+Na]^+$, 1699.6 $[M+K]^+$; elemental analysis calcd (%) for $C_{105}H_{117}N_3O_{15}$: C 75.92, H 7.10, N 2.53; found: C 76.01, H 7.22, N 2.45.

Synthesis of Calix[6]arene (6)

In a 100 mL round-bottom flask kept under a nitrogen atmosphere, a tip of spatula of Pd/C catalyst was cautiously added to a suspension of compound **5** (0.40 g, 0.25 mmol) in methanol (50 mL), then hydrazine monohydrate (1.03 g, 20 mmol) was added dropwise. The resulting heterogeneous mixture was heated at reflux for 6 h, cooled to room temperature, and then filtered, under a nitrogen atmosphere, through a Celite pad to remove the Pd/C catalyst. The filtered solution was evaporated to dryness under reduced pressure to yield 0.38 g of **6** (98%) as a white solid. Because of its instability to air, compound **6** was employed in the following synthetic step without any further purification.

Synthesis of the "Naphtho" Calix[6]arene-based Wheel (7)

In a 50 mL round-bottom flask kept under a nitrogen atmosphere, phenyl isocyanate (0.18 g, 1.44 mmol) was added dropwise to a solution of **6** (0.38 g, 0.24 mmol) in dichloromethane (20 mL). The reaction mixture was stirred for two hours at room temperature, then the solvent was evaporated to dryness under reduced pressure, and the residue was purified by column chromatography on silica gel (hexane/ethyl acetate 65:35) to yield 0.18 g of **7** (38%) as a pale-yellow solid. M.p. = 147–149 °C; ^{1}H NMR ($CDCl_3$, 400 MHz): δ = 7.78–7.61 (m, 9H), 7.44 (t, 3H, J = 7.8 Hz), 7.33 (t, 3H, J = 7.8 Hz), 7.23 (s, 6H), 7.15 (d, 3H, J = 2.4 Hz), 7.13 (s, 6H), 7.11–7.10 (m, 15H), 6.96–6.93 (m, 3H), 6.30 (s, 6H), 4.42 (d, 6H, J = 15.6 Hz), 4.12 (t, 6H, J = 15.2 Hz), 2.82 (s, 9H), 1.93 (q, 12H, J = 7.2 Hz), 1.7 (bs, 12H), 1.32–1.27 ppm (ms, 27H); ^{13}C NMR (100 MHz): δ = 157.1, 155.0, 154.6, 152.3, 146.8, 138.2, 135.7, 134.6, 133.0, 132.4, 129.3, 129.1, 129.0, 128.9, 127.7, 127.6, 126.7, 126.3, 123.5, 123.4, 123.1, 120.6, 119.0, 107.7, 106.6, 72.8, 67.9, 60.2, 34.2, 31.5, 31.1, 30.5, 29.7, 29.2, 26.2, 26.1 ppm; MS (ESI) *m/z*: 1951.3 $[M+Na]^+$, 1967.2 $[M+K]^+$; elemental analysis calcd (%) for $C_{126}H_{138}N_6O_{12}$: C 78.47, H 7.21, N 4.36; found: C 77.41, H 7.31, N 4.23.

Synthesis of the "Naphtho" Calix[6]arene-based Wheel (10)

In a 100 mL round-bottom flask, under a nitrogen atmosphere, a tip of spatula of Pd/C catalyst was cautiously added to a suspension of **8** (0.30 g, 0.25 mmol) and hydrazine monohydrate (1.03 g, 20 mmol) in methanol (50 mL). After refluxing overnight, the reaction mixture was filtered, under a nitrogen atmosphere, through a Celite pad to remove the catalyst. The filtered solution was evaporated to dryness and the residue taken up with dichloromethane (25 mL). To the resulting homogeneous solution, α-naphthyl isocyanate **9** (0.23 g, 1.25 mmol) was added dropwise. The reaction mixture was stirred for two hours at room temperature, then the solvent was evaporated to dryness under reduced pressure, and the residue was purified by column chromatography on silica gel (hexane/ethyl acetate 6:4) to yield 0.23 g of **10** (48%) as a purple solid. M.p. = 162–163 °C; ^{1}H NMR ($CDCl_3$, 400 MHz): δ = 7.5 (bs, 9H), 7.4 (bs, 3H), 7.2 (bs, 15H), 7.0 (bs, 3H), 6.8 (bs, 3H), 6.5 (bs, 6H), 4.5 (bs, 6H), 4.2 (bs, 6H), 3.9 (bs, 6H), 3.68–3.62 (ms, 12H), 2.8 (bs, 9H), 1.28–1.24 ppm (ms, 36H); ^{13}C NMR (100 MHz): δ = 155.9, 154.7, 146.6, 135.9, 133.9, 133.1, 128.0, 127.9, 127.8, 125.8, 125.6, 125.4, 125.0, 123.4, 121.3, 120.7, 72.3, 69.3, 66.9, 60.2, 34.2, 31.5, 31.10 ppm; MS (ESI) *m/z*: 1638.7 $[M+Na]^+$, 1654.7 $[M+K]^+$; elemental analysis calcd (%) for $C_{102}H_{114}N_6O_{12}$: C 75.81, H 7.11, N 5.20; found: C 75.20, H 7.20, N 4.99.

Acknowledgments

This project has received funding from the European Research Council (ERC) under the European Union's Horizon 2020 research and innovation programme (grant agreement No. 692981), the Italian MIUR (PRIN 2010CX2TLM), and the Universities of Bologna and Parma. We thank CIM (Centro Interdipartimentale di Misure) "G. Casnati" of the University of Parma for NMR and MS measurements.

Keywords: calixarenes · fluorescence spectroscopy · naphthyl ureas · pseudorotaxanes · viologens

[1] T. Nakamura, T. Matsumoto, H. Tada, K. Sugiura, *Chemistry of Nanomolecular Systems: Towards the Realization of Molecular Devices*, Springer, Berlin, **2003**.
[2] S. Saha, J. F. Stoddart, *Chem. Soc. Rev.* **2007**, *36*, 77–92.
[3] V. Balzani, A. Credi, M. Venturi, *Molecular Devices and Machines: Concepts and Perspectives for the Nanoworld*, Wiley-VCH, Weinheim, **2008**.
[4] P. A. Gale, J. W. Steed, *Supramolecular Chemistry: From Molecules to Nanomaterials*, John Wiley & Sons, Chichester, **2012**.
[5] S. F. M. van Dongen, S. Cantekin, J. A. A. W. Elemans, A. E. Rowan, R. J. M. Nolte, *Chem. Soc. Rev.* **2014**, *43*, 99–122.
[6] P. Ceroni, A. Credi, M. Venturi, *Chem. Soc. Rev.* **2014**, *43*, 4068–4083.
[7] L. Prodi, *New J. Chem.* **2005**, *29*, 20–31.
[8] B. Daly, J. Ling, A. P. de Silva, *Chem. Soc. Rev.* **2015**, *44*, 4203–4211.
[9] B. L. Feringa, W. R. Browne, *Molecular Switches*, Wiley-VCH, Weinheim, **2011**.
[10] A. C. Benniston, *Chem. Soc. Rev.* **2004**, *33*, 573–578.
[11] H. Tian, Q.-C. Wang, *Chem. Soc. Rev.* **2006**, *35*, 361–374.
[12] W. Yang, Y. Li, H. Liu, L. Chi, Y. Li, *Small* **2012**, *8*, 504–516.
[13] G. Yu, C. Han, Z. Zhang, J. Chen, X. Yan, B. Zheng, S. Liu, F. Huang, *J. Am. Chem. Soc.* **2012**, *134*, 8711–8717.
[14] G. Yu, M. Xue, Z. Zhang, J. Li, C. Han, F. Huang, *J. Am. Chem. Soc.* **2012**, *134*, 13248–13251.
[15] G. Yu, X. Zhou, Z. Zhang, C. Han, Z. Mao, C. Gao, F. Huang, *J. Am. Chem. Soc.* **2012**, *134*, 19489–19497.
[16] V. Balzani, M. Gomez-Lopez, J. F. Stoddart, *Acc. Chem. Res.* **1998**, *31*, 405–414.
[17] V. Balzani, A. Credi, M. Venturi, *Chem. Soc. Rev.* **2009**, *38*, 1542–1550.
[18] A. K. Mandal, M. Gangopadhyay, A. Das, *Chem. Soc. Rev.* **2015**, *44*, 663–676.
[19] W. R. Browne, B. L. Feringa, *Nat. Nanotechnol.* **2006**, *1*, 25–35.
[20] J.-P. Sauvage, P. Gaspard, *From Non-Covalent Assemblies to Molecular Machines*, Wiley-VCH, Weinheim, **2010**.
[21] A. Arduini, R. Ferdani, A. Pochini, A. Secchi, F. Ugozzoli, *Angew. Chem. Int. Ed.* **2000**, *39*, 3453–3456; *Angew. Chem.* **2000**, *112*, 3595–3598.
[22] F. Ugozzoli, C. Massera, A. Arduini, A. Pochini, A. Secchi, *CrystEngComm* **2004**, *6*, 227–232.
[23] A. Credi, S. Dumas, S. Silvi, M. Venturi, A. Arduini, A. Pochini, A. Secchi, *J. Org. Chem.* **2004**, *69*, 5881–5887.

[24] A. Arduini, R. Bussolati, A. Credi, G. Faimani, S. Garaudée, A. Pochini, A. Secchi, M. Semeraro, S. Silvi, M. Venturi, *Chem. Eur. J.* **2009**, *15*, 3230 – 3242.
[25] A. Arduini, R. Bussolati, D. Masseroni, G. Royal, A. Secchi, *Eur. J. Org. Chem.* **2012**, 1033 – 1038.
[26] A. Arduini, R. Bussolati, A. Credi, S. Monaco, A. Secchi, S. Silvi, M. Venturi, *Chem. Eur. J.* **2012**, *18*, 16203 – 16213.
[27] A. Arduini, R. Bussolati, A. Credi, A. Secchi, S. Silvi, M. Semeraro, M. Venturi, *J. Am. Chem. Soc.* **2013**, *135*, 9924 – 9930.
[28] J. S. Kim, D. T. Quang, *Chem. Rev.* **2007**, *107*, 3780 – 3799.
[29] M. Suresh, A. K. Mandal, M. K. Kesharwani, N. N. Adarsh, B. Ganguly, R. K. Kanaparthi, A. Samanta, A. Das, *J. Org. Chem.* **2011**, *76*, 138 – 144.
[30] M. Suresh, A. K. Mandal, E. Suresh, A. Das, *Chem. Sci.* **2013**, *4*, 2380 – 2386.
[31] A. Arduini, F. Calzavacca, A. Pochini, A. Secchi, *Chem. Eur. J.* **2003**, *9*, 793 – 799.
[32] A. Arduini, F. Ciesa, M. Fragassi, A. Pochini, A. Secchi, *Angew. Chem. Int. Ed.* **2005**, *44*, 278 – 281; *Angew. Chem.* **2005**, *117*, 282 – 285.
[33] A. Casnati, L. Domiano, A. Pochini, R. Ungaro, M. Carramolino, J. Oriol Magrans, P. M. Nieto, J. López-Prados, P. Prados, J. de Mendoza, R. G. Janssen, W. Verboom, D. N. Reinhoudt, *Tetrahedron* **1995**, *51*, 12699 – 12720.
[34] J. J. González, R. Ferdani, E. Albertini, J. M. Blasco, A. Arduini, A. Pochini, P. Prados, J. de Mendoza, *Chem. Eur. J.* **2000**, *6*, 73 – 80.
[35] A. Credi, L. Prodi, *J. Mol. Struct.* **2014**, *1077*, 30 – 39.
[36] J. R. Lakowicz, *Principles of Fluorescence Spectroscopy*, Springer US, Boston, MA, **2006**.
[37] V. Balzani, P. Ceroni, A. Juris, *Photochemistry and Photophysics: Concepts, Research, Applications*, Wiley-VCH, Weinheim, **2014**.
[38] D. Rehm, A. Weller, *Isr. J. Chem.* **1970**, *8*, 259 – 263.
[39] V. Balzani, *Electron Transfer in Chemistry*, Wiley-VCH, Weinheim, **2001**.
[40] A. Arduini, R. Bussolati, A. Credi, A. Pochini, A. Secchi, S. Silvi, M. Venturi, *Tetrahedron* **2008**, *64*, 8279 – 8286.
[41] A. Arduini, A. Credi, G. Faimani, C. Massera, A. Pochini, A. Secchi, M. Semeraro, S. Silvi, F. Ugozzoli, *Chem. Eur. J.* **2008**, *14*, 98 – 106.
[42] V. Balzani, P. Ceroni, A. Credi, M. Gómez-López, C. Hamers, J. F. Stoddart, R. Wolf, *New J. Chem.* **2001**, *25*, 25 – 31.
[43] H. Qian, D. S. Guo, Y. Liu, *Chem. Eur. J.* **2012**, *18*, 5087 – 5095.
[44] A. Bouzide, G. Sauvé, *Org. Lett.* **2002**, *4*, 2329 – 2332.
[45] M. Montalti, A. Credi, L. Prodi, M. T. Gandolfi, *Handbook of Photochemistry*, CRC/Taylor & Francis, Boca Raton, FL, **2006**.
[46] R. A. Binstead, *SPECFIT*/32, Spectrum Software Associates, Chapel Hill, NC, **1996**.
[47] N. G. Connelly, W. E. Geiger, *Chem. Rev.* **1996**, *96*, 877 – 910.

Received: October 17, 2016
Published online on January 9, 2017

